



Cite this: DOI: 10.1039/d0nj05978a

Development of a continuous-flow tubular reactor for synthesis of 5-hydroxymethylfurfural from fructose using heterogeneous solid acid catalysts in biphasic reaction medium†

 Sadra Souzanchi,^a Laleh Nazari,^a Kasanneni Tirumala Venkateswara Rao,^{*a} Zhongshun Yuan,^a Zhongchao Tan^{*b} and Chunbao Charles Xu ^{*a}

5-Hydroxymethylfurfural (5-HMF) is an important biomass-derived platform chemical used to produce polymers, biofuels, and other valuable industrial chemicals. In this work, 5-HMF was synthesized from biomass-derived fructose through a continuous flow process using heterogeneous solid acid catalysts. Different solid acid catalysts, including niobium-based catalysts, Amberlyst 15, and Amberlyst 36, were tested for selective dehydration of fructose to 5-HMF in a biphasic (H₂O/MIBK) continuous-flow tubular reactor. The catalysts were characterized using complementary techniques, including BET surface area, XRD, TGA, NH₃-TPD, FT-IR, and pyridine-FT-IR. We also studied the effects of different reaction parameters such as the initial fructose concentration, reaction temperature, feeding flow rate, and aqueous-to-organic phase ratio. The optimal conditions were determined to be 150 °C temperature, a 0.25 ml min⁻¹ feeding flow rate, 200 mg ml⁻¹ NaCl concentration, 200 and 400 mg ml⁻¹ fructose concentrations, and aqueous-to-organic phase ratios of 1:5 and 1:10. In addition, niobium phosphate (NbP), synthetic sulphated niobia (NbS) and Amberlyst 36 (Amb. 36) were active and selective, leading to 5-HMF yields in the range of 54–60% under the optimal operating conditions. Meanwhile, the Amb. 36 catalyst exhibited a 5-HMF selectivity of 70% at 150 °C, and therefore it was selected as the catalyst for the fructose dehydration reaction. Additionally, the Amb. 36 catalyst showed consistent catalytic activity and selectivity during a time-on-stream of 8 h. Furthermore, a reusability test with the used catalyst demonstrated that this catalyst can be recycled and reused without losing its catalytic activity.

 Received 7th December 2020,
 Accepted 30th March 2021

DOI: 10.1039/d0nj05978a

rsc.li/njc

1. Introduction

Over the past decade, the production of chemicals and fuels from alternative resources has attracted much attention because of the fast dwindling of fossil deposits and environmental issues associated with the continuous use of petroleum reserves.^{1,2} 5-Hydroxymethylfurfural (5-HMF) is one of the top-value-added bio-based intermediate platform chemicals that can be directly produced from lignocellulosic biomass by depolymerization, followed by a dehydration reaction.³ 5-HMF can be used to synthesize various industrially useful chemicals and fuels by oxidation,⁴ amination,^{5,6} aldol condensation,^{7,8} and hydrogenation reactions.^{9,10} Particularly, 5-HMF can be used to synthesize 2,5-furandicarboxylic acid (FDCA)^{11–13} which can replace the

petroleum-based terephthalic acid in the production of polyethylene furanoate (PEF) polymer for bottle and packaging applications.^{14,15} In addition, 5-HMF also can be used in the preparation of formaldehyde-free phenol-5-hydroxymethylfurfural (PHMF) resin, which is an alternative to the conventional Novolac PF resin.^{16,17}

Although the most economical hexose is glucose as a key component of cellulosic biomass, fructose has proven to be a more favorable feedstock than glucose for 5-HMF production as it gives higher yields of 5-HMF.¹⁸ On the one hand, glucose has a more stable ring structure than fructose does, and the formation of 5-HMF from hexoses proceeds through an open-chain mechanism. A low fraction of open chain that is formed in solution when glucose is used as a feedstock can result in low enolization rates.^{18,19} Glucose first isomerizes to fructose before its conversion to 5-HMF. As the isomerization process is *via* alkali-catalyzed reactions, high yields of 5-HMF from glucose in acidic media are not expected.¹⁸

Several studies have reported the production of 5-HMF from fructose and glucose in various solvents with different acidic catalysts, either homogeneous or heterogeneous.^{20–25} Among the

^a Department of Chemical and Biochemical Engineering, Western University, London, Ontario, N6A 5B9, Canada. E-mail: venkat.kasanneni@gmail.com, cxu6@uwo.ca

^b Department of Mechanical & Mechatronics Engineering, University of Waterloo, Waterloo, ON, N2L 3G1, Canada. E-mail: tanz@uwaterloo.ca

† Electronic supplementary information (ESI) available. See DOI: 10.1039/d0nj05978a

possible reaction media, water is considered the most economical and environmentally-friendly. The application of heterogeneous catalysts is also favourable because of their recyclability, thus facilitating an environmentally-friendly and cost-effective conversion. Moreover, heterogeneous catalysts have shown superior 5-HMF selectivity.²⁶ However, most of the solid acid catalysts cannot maintain their acidity in water without deactivation of their acid sites, and they have low 5-HMF yields even at high reaction temperatures in addition to low selectivity because of the uncontrolled rehydration of 5-HMF to levulinic and formic acids and/or the self-polymerization of 5-HMF leads to the formation of soluble and insoluble polymeric substances called humins.^{27–29} One of the proposed solutions to this problem is the *in situ* extraction of 5-HMF from the aqueous reaction media using an organic extractive solvent, which is immiscible in water to avoid its successive transformation.^{18,29} Efforts have been made to improve the 5-HMF yield in the dehydration of fructose/glucose with a water-immiscible low-boiling organic solvent to extract the 5-HMF formed from the reacting phase. Different organic solvents such as methyl isobutyl ketone (MIBK), tetrahydrofuran (THF), *n*-butanol, γ -valerolactone (GVL), and 2-methyl tetrahydrofuran (2-MeTHF) have been used to improve the 5-HMF yield.^{30–33} Furthermore, addition of NaCl salt to the biphasic reaction medium results in the salting-out effect, which further enhances the 5-HMF yield.³¹

Both niobic acid ($\text{Nb}_2\text{O}_5 \cdot n\text{H}_2\text{O}$) and niobium phosphate (NbOPO_4) contain Brønsted and Lewis acid sites and are well known as water-tolerant bifunctional heterogeneous solid acid catalysts for different catalytic reactions, especially for the conversion of sugars to 5-HMF and furfural.^{28,34,35} Zhang *et al.* have studied the performance of a series of porous niobium phosphate solid acid catalysts for the conversion of glucose or glucose-united carbohydrates into 5-HMF in pure water and water/MIBK solvent mixtures.³⁶ They find that the niobium phosphate catalyst contains both Lewis acid and Brønsted acid sites, which are effective in isomerizing glucose to fructose and dehydrating fructose to 5-HMF, respectively. Under the optimum operating conditions and in the presence of a niobium phosphate catalyst, 33.2% and 39.3% 5-HMF yields were obtained from glucose in pure water and water/MIBK solvents, respectively.³⁶ In another study by Carlini *et al.*, the dehydration of fructose, sucrose and inulin to 5-HMF is studied by using niobium-based catalysts in an aqueous medium. All the examined niobium catalysts display higher activities than other heterogeneous systems do under similar operating conditions.³⁷ H_3PO_4 -Treated niobic acid has a lower selectivity at a higher substrate conversion than niobium phosphate catalysts do, which results from the slightly higher Lewis and Brønsted acid sites for the niobium phosphate. Improvement in the activity and selectivity of the catalysts was observed when 5-HMF was extracted with MIBK from the aqueous media.³⁷ Apart from the niobium based catalysts, various other heterogeneous catalysts such as vanadyl pyrophosphate,³⁸ TPA-AC,³⁹ $\text{SO}_4^{2-}/\text{TiO}_2$,⁴⁰ mesoporous ZrO_2 nanopowder,⁴¹ arene sulfonic acid-functionalized metal-organic framework (MOF),⁴² functionalized nano graphitic carbon,⁴³ and functionalized zeolite catalyst⁴⁴ have been tested for the conversion of fructose to 5-HMF.

All these catalysts exhibit moderate to high 5-HMF yields under various reaction conditions using different reaction media.

Furthermore, polystyrene sulfonic acid resins act as solid Brønsted acids and these catalysts can also be used for the dehydration of fructose to 5-HMF. Simeonov *et al.* reported Amberlyst-15 catalyst for the dehydration of fructose in a tetraethylammonium bromide reaction medium at 100 °C for 15 min and obtained 97% isolated yield of 5-HMF with 99% purity.⁴⁵ In other work, Antonetti *et al.* use an Amberlyst-70 catalyst for the production of 5-HMF from a highly concentrated solution of fructose (10 and 20 wt%) and achieve a more than 46% molar yield of 5-HMF at 180 °C.⁴⁶ Qi *et al.* reported Amberlyst-15 catalyst for fructose dehydration into 5-HMF in ionic liquid 1-butyl-3-methyl imidazolium chloride. A fructose conversion of 98.6% and a 5-HMF yield of 82.2% were achieved at 80 °C.²⁴ Although these catalysts are highly selective in batch processes, it is necessary to evaluate their performance in a continuous mode of fructose dehydration.

So far, most 5-HMF production reactions have been performed in batch reactors^{26,28,29,47} or continuous stirred tank reactors (CSTR).^{48–50} Continuous plug flow reactors (PFR) can offer lower operating costs and lower environmental impacts of chemical production compared with batch reactors.⁵¹ They also can vary the reaction time and alter the product properties by changing the feeding flow rate and/or catalyst loading. In addition, they could be a better mode for large-scale operations. There are few studies on the continuous flow dehydration of hexoses into 5-HMF using plug flow reactors in single-phase⁵² or biphasic media using a microscale reactor with a homogeneous catalyst,^{51,53–55} and metal oxide particles, metal phosphates, ion exchange resins and mesoporous organosilicas as heterogeneous catalysts.^{56–59} Since continuous-flow reactors are more desirable for industrial and commercial production, more comprehensive studies are needed to optimize the operating conditions for the continuous production of 5-HMF.

In this study, we report a home-made continuous-flow tubular reactor for the biphasic dehydration of fructose to 5-HMF using niobium compounds and ion exchange resins as solid acid catalysts. To the best of our knowledge, these catalysts have not been tested for the dehydration of fructose to 5-HMF in a biphasic continuous-flow tubular reactor. The catalysts were characterized using complementary technologies, including TGA, XRD, TPD-NH₃, BET/PSD, FT-IR and Py-FTIR analyses to examine their fructose conversion, 5-HMF selectivity, and 5-HMF yield. The effects of different operating conditions, such as the reaction temperature, feeding flow rate, initial fructose concentration, aqueous-to-organic phase ratio (A/O), and phase transfer catalyst (PTC), on different catalysts are studied to determine the optimal conditions for 5-HMF production.

2. Materials and methods

2.1 Materials

D-Fructose (>99%), Amberlyst 15, Amberlyst 36, triethylamine (TEA), sodium chloride (NaCl) and 5-hydroxymethylfurfural

(99%, for preparing HPLC standard solution) were purchased from Sigma-Aldrich. Niobic acid ($\text{Nb}_2\text{O}_5 \cdot n\text{H}_2\text{O}$), and niobium phosphate hydrate ($\text{NbOPO}_4 \cdot n\text{H}_2\text{O}$) were supplied by CBMM (Companhia Brasileira de Metalurgia e Mineração). HPLC grade water and acetonitrile for preparing the mobile phase for HPLC analysis as well as methyl isobutyl ketone (MIBK) were purchased from Caledon Laboratory Chemicals and used as received.

2.2 Catalyst preparation

The powdered catalysts were pelletized for using powdered catalysts in a plug flow reactor as a packed catalytic bed. Niobium phosphate (hereafter named as NbP) and niobic acid (hereafter named as NbA) powders were humidified overnight and then pressed in a pellet die using a hydraulic press at 10 tonnes per cm^2 of pressure to create pellets. The pellets were then crushed using a Wiley Mill and sieved; particles of sizes between 420 and 840 μm (mesh no. 40 to mesh no. 20) were collected and used for the experiments. Synthesized phosphated niobia (named as NbP-syn in this study) and synthesized

sulphated niobia (named as NbS-syn) were prepared by wet impregnation of 100 g niobic acid powder in 1 litre of phosphoric acid and sulfuric acid solutions in water (1 M), respectively. The solutions were first mixed using a magnetic stirrer for 24 hours, then filtered, and finally dried overnight at 105 $^\circ\text{C}$ in an oven. The dried powders were then pelletized following the same procedure as that for NbA and NbP. Amberlyst 15 (hereafter named as Amb. 15) and Amberlyst 36 beads (hereafter named as Amb. 36) were used as received.

2.3 Continuous-flow reactor setup and experimental procedure

The catalytic conversion of fructose to 5-HMF was performed in a novel biphasic continuous-flow tubular reactor, which is presented in Fig. 1. The lab-scale tubular reactor was home-made for testing different heterogeneous solid catalysts as a fixed bed within the tubular reactor for the conversion of sugars to 5-HMF. For a typical test, pure fructose solution in an aqueous medium was used as the feedstock, and MIBK was used as the extracting organic solvent. MIBK could be used for the continuous

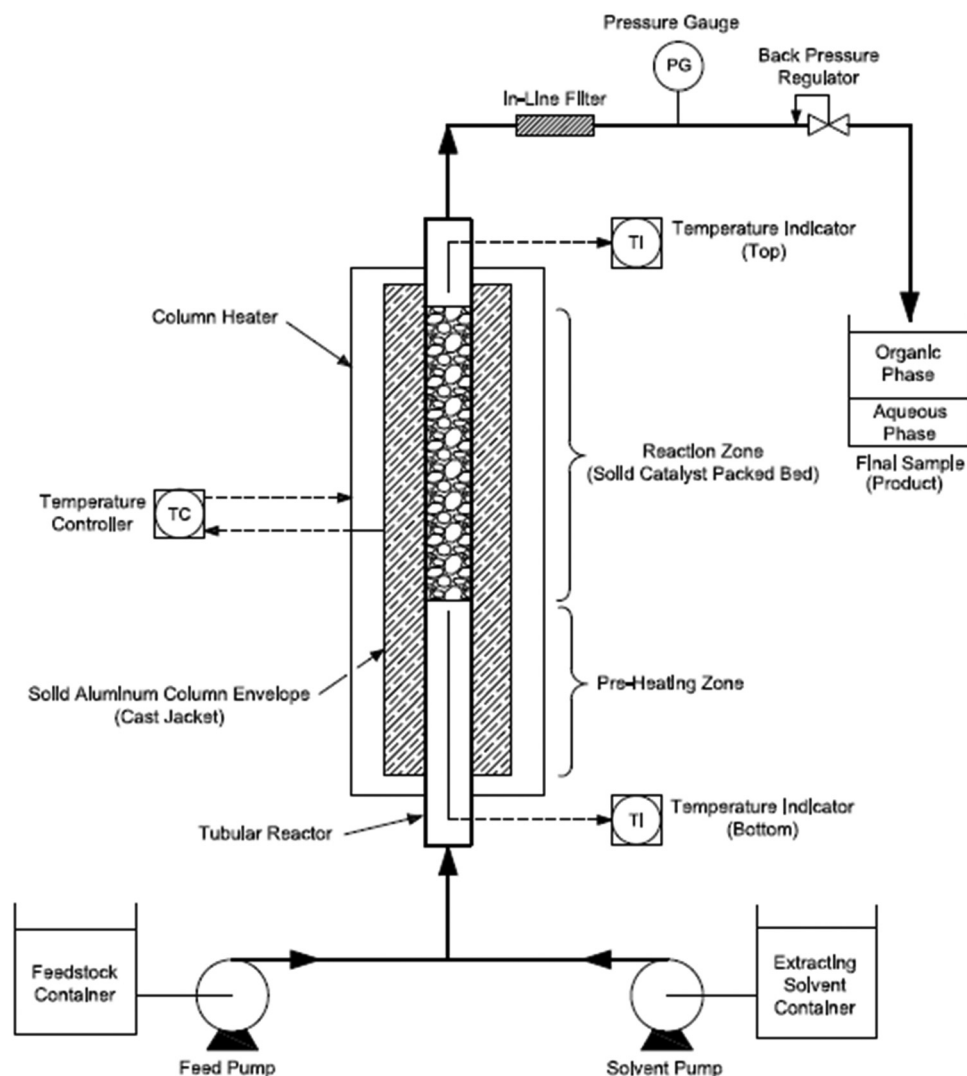


Fig. 1 Schematic diagram of the biphasic continuous-flow tubular reactor system.

in-situ extraction of the produced 5-HMF from the aqueous medium inside the fixed-bed catalytic reactor to enhance the 5-HMF selectivity and yield by suppressing the side reactions of 5-HMF in water. In addition, sodium chloride (NaCl) was added to the aqueous phase of the feedstock to enhance the partition coefficient of 5-HMF towards the organic phase (*via* the salting-out effect).

This reactor setup mainly consists of a vertical tubular reactor (SS-316 1/2" or 5/8" tubes, 30 cm long) seamlessly fitted inside a custom-manufactured bipartite solid aluminum column envelope connected to a heat generator surface inside a column heater (Eppendorf CH-30). The column envelope is made of aluminum because of its high thermal conductivity for uniform heat transfer from the heater to the tubular reactor. In the column heater, the temperature of the heat generator surface is adjusted and controlled using a temperature controller (Eppendorf TC-50); hence the aluminum column envelope can keep the temperature constant and uniform along the tubular reactor.

In a typical operation, an appropriate amount of heterogeneous solid catalyst (with particle sizes between 420 and 840 μm) is preloaded and supported inside the tubular reactor as a packed bed between two quartz wool plugs at the upper 2/3 length of the reactor (20 cm, reaction zone); the lower 1/3 length of the reactor (10 cm, pre-heating zone) remains empty to pre-heat the flowing biphasic media to the predetermined reaction temperature before entering the reaction zone. Two HPLC feeding pumps (SSI Mighty Mini Pump) connected to the bottom of the tubular reactor provide independent and adjustable flow rates of the aqueous feedstock solutions (containing substrate sugar, NaCl and water) and extracting organic solvent (pure MIBK) and then two phases are mixed in a tee union to provide a uniform upward rising flow of biphasic media through the tubular reactor. Meanwhile, the temperature of the flowing biphasic media before and after passing the catalyst bed is monitored using two thermocouples (Omega 1/8" K-type) located at upstream and downstream of the reaction zone (catalyst bed) inside the tubular reactor; the thermocouples are connected to a digital thermometer. The pressure of the flowing media inside the reactor is adjusted and controlled using a back pressure regulator valve (Swagelok KBP Series) located on the exit line of the reactor, and the pressure of the system is monitored using a pressure gauge.

In a typical run, after a specific amount of the heterogeneous solid catalyst particles (depending on the bulk density of the catalyst needed to completely fill the reaction zone) had been preloaded inside the tubular reactor as a packed bed and the reactor had been assembled inside the column heater within the aluminum column envelope, the aqueous feedstock solution was pumped into the reactor using the dedicated feeding pump at a specific flow rate. When the reactor is filled up with feedstock solution, the extracting organic solvent (MIBK) is concurrently pumped at a specific flow rate to the reactor. Then, the pressure inside the reactor is raised to the desired pressure (typically 10 bar) using the backpressure regulator valve to avoid boiling of the water at the reaction temperatures above 100 $^{\circ}\text{C}$ and the formation of vapour bubbles within the reactor system. The reactor is then heated to the desired temperature after insulating the column heater and tubular reactor. After the reactor reaches a stable

temperature at the set-point and steady-state conditions (depending on the feeding flow rate), samples are taken every hour, and each phase (aqueous or organic) fractionated from the sample is separately analyzed using HPLC. The concentrations of fructose and 5-HMF in each phase are calculated using data from the HPLC chromatographs. The time on stream (TOS) for all experiments is 8 hours, and no detectable soluble by-product or any other intermediate is found in the HPLC chromatographs.

2.4 Product analyses

Each phase (organic and aqueous) of the product samples collected from the experiments is separately analyzed using an HPLC instrument (Waters 2690 Separation Module) equipped with both an RI detector (Waters 410 Differential Refractometer) with an internal detector temperature of 35 $^{\circ}\text{C}$ and a UV detector (Waters 484 Tunable Absorbance Detector) set at 284 nm to determine the amount of feedstock (fructose) consumed and the amount of product (5-HMF) produced, respectively. A Waters XBridge Amide column (3.5 μm , 4.6 \times 250 mm) maintained at 35 $^{\circ}\text{C}$ is used, and the mobile phase is 75/25 acetonitrile/water (v/v) with 0.2 v% triethylamine (TEA) at a flow rate of 0.6 ml min^{-1} . The results for all experiments are analyzed by external calibration curves generated for fructose and 5-HMF separately using standard solutions of fructose and 5-HMF of known concentrations. The results are reported in terms of the conversion, selectivity, and yield, which are defined and calculated as follows:

$$\begin{aligned} \text{Fructose conversion (\%)} &= \frac{\left[\left(C_{\text{Fru}}^{\text{aqu,F}} \times Q^{\text{aqu}} \right) - \left(C_{\text{Fru}}^{\text{aqu,P}} \times Q^{\text{aqu}} \right) \right] / M_{\text{Fru}}}{\left(C_{\text{Fru}}^{\text{aqu,F}} \times Q^{\text{aqu}} \right) / M_{\text{Fru}}} \times 100\% \\ &= \frac{C_{\text{Fru}}^{\text{aqu,F}} - C_{\text{Fru}}^{\text{aqu,P}}}{C_{\text{Fru}}^{\text{aqu,F}}} \times 100\% \end{aligned} \quad (5.1)$$

$$\begin{aligned} \text{HMF selectivity (\%)} &= \frac{\left[\left(C_{\text{HMF}}^{\text{aqu,P}} \times Q^{\text{aqu}} \right) + \left(C_{\text{HMF}}^{\text{org,P}} \times Q^{\text{org}} \right) \right] / M_{\text{HMF}}}{\left[\left(C_{\text{Fru}}^{\text{aqu,F}} \times Q^{\text{aqu}} \right) - \left(C_{\text{Fru}}^{\text{aqu,P}} \times Q^{\text{aqu}} \right) \right] / M_{\text{Fru}}} \times 100\% \\ &= \frac{\left[C_{\text{HMF}}^{\text{aqu,P}} + \left(C_{\text{HMF}}^{\text{org,P}} \times \frac{Q^{\text{org}}}{Q^{\text{aqu}}} \right) \right] / M_{\text{HMF}}}{\left(C_{\text{Fru}}^{\text{aqu,F}} - C_{\text{Fru}}^{\text{aqu,P}} \right) / M_{\text{Fru}}} \times 100\%. \end{aligned} \quad (5.2)$$

$$\begin{aligned} \text{Total HMF yield (\%)} &= \frac{\left[\left(C_{\text{HMF}}^{\text{aqu,P}} \times Q^{\text{aqu}} \right) + \left(C_{\text{HMF}}^{\text{org,P}} \times Q^{\text{org}} \right) \right] / M_{\text{HMF}}}{\left(C_{\text{Fru}}^{\text{aqu,F}} \times Q^{\text{aqu}} \right) / M_{\text{Fru}}} \times 100\% \\ &= \frac{\left[C_{\text{HMF}}^{\text{aqu,P}} + \left(C_{\text{HMF}}^{\text{org,P}} \times \frac{Q^{\text{org}}}{Q^{\text{aqu}}} \right) \right] / M_{\text{HMF}}}{C_{\text{Fru}}^{\text{aqu,F}} / M_{\text{Fru}}} \times 100\% \end{aligned}$$

where, $C_{\text{Fructose}}^{\text{aq},\text{F}}$ is the mass concentration of fructose in the aqueous feedstock solution (mg ml^{-1}), $C_{\text{Fructose}}^{\text{aq},\text{P}}$ is the mass concentration of fructose in the aqueous phase of the product sample (mg ml^{-1}), $C_{\text{HMF}}^{\text{aq},\text{P}}$ is the mass concentration of HMF in the aqueous phase of the product sample (mg ml^{-1}), $C_{\text{HMF}}^{\text{org},\text{P}}$ is the mass concentration of HMF in the organic phase of the product sample (mg ml^{-1}), Q^{aq} is the volumetric flow rate of the aqueous feedstock solution (ml min^{-1}), Q^{org} is the volumetric flow rate of the extracting organic solvent (ml min^{-1}), M_{Fructose} is the molar mass of fructose ($= 180.16 \text{ g mol}^{-1}$), and M_{HMF} is the molar mass of HMF ($= 126.11 \text{ g mol}^{-1}$).

2.5 Catalyst characterization methods

The Brunauer–Emmett–Teller (BET) surface area, as well as the pore volume and pore size distribution (PSD) measurements, are measured using a Micrometrics Tristar II 3020 series instrument. The samples are initially degassed under nitrogen flow for 8 hours at $110 \text{ }^\circ\text{C}$. The crystalline phases and structure of the catalyst samples were investigated by X-ray diffraction (XRD) on a PANalytical X'Pert Pro diffractometer using Cu-K α radiation.

The total acidity of the catalysts is measured by temperature-programmed desorption of ammonia (TPD-NH₃). TPD-NH₃ is analyzed using a ChemBET Pulsar TPR/TPD automated chemisorption analyzer. In a typical experiment, about 1 mg of the catalyst sample is pretreated in a quartz reactor at $300 \text{ }^\circ\text{C}$ for 1 hour with flowing helium (99.9%, 120 ml min^{-1}) to remove the physically adsorbed substances. After pretreatment, the sample is saturated with anhydrous ammonia at $100 \text{ }^\circ\text{C}$ for 10 minutes, and subsequently it is flushed with helium at the same temperature to remove any physisorbed ammonia. Then, TPD analysis is carried out by heating the catalyst sample from ambient temperature to $800 \text{ }^\circ\text{C}$ with a heating rate of $10 \text{ }^\circ\text{C min}^{-1}$, during which the desorbed ammonia is measured by thermal conductivity detector (TCD) within the temperature range of $100\text{--}800 \text{ }^\circ\text{C}$.

Fourier transform infrared (FT-IR) spectrometry analyses of the catalyst samples are conducted using a PerkinElmer FT-IR spectrometer, and the spectra are recorded in the region of $4000\text{--}550 \text{ cm}^{-1}$. The FT-IR spectra with adsorbed pyridine (Py-FTIR) are in the range of $1600\text{--}1400 \text{ cm}^{-1}$. Before pyridine adsorption, 1 g of each catalyst sample is heated in a vacuum oven at $150 \text{ }^\circ\text{C}$ overnight to be degassed and then cooled to room temperature in a desiccator. 500 mg of each degassed sample is separated at this stage and is used as the background reference for the corresponding pyridine adsorbed sample. Another 500 mg of each sample is then treated with 500 μl of pyridine and degassed again in a vacuum oven at $150 \text{ }^\circ\text{C}$ for 4 hours to remove physically adsorbed pyridine. The spectra are recorded in the region of $1600\text{--}1400 \text{ cm}^{-1}$ after the samples have been cooled to ambient temperature. The Brønsted acid to Lewis acid site ratio (B/L) for each catalyst is evaluated by the ratio of the peak areas at 1540 cm^{-1} and 1445 cm^{-1} , which are attributed to the characteristic peaks for pyridine adsorbed on Brønsted acid and Lewis acid sites, respectively.⁶⁰

Thermogravimetric analysis (TGA) of the fresh catalysts is conducted using a PerkinElmer Pyris 1 TGA instrument in a

nitrogen atmosphere. The samples are heated in a nitrogen flow at 20 ml min^{-1} from $40 \text{ }^\circ\text{C}$ to $100 \text{ }^\circ\text{C}$ at $10 \text{ }^\circ\text{C min}^{-1}$ and then kept at $100 \text{ }^\circ\text{C}$ for 10 min to remove the adsorbed moisture and volatile compounds. Then they are heated to $700 \text{ }^\circ\text{C}$ at a heating rate of $10 \text{ }^\circ\text{C min}^{-1}$, and the change in the sample weight by temperature is recorded. For the spent catalyst, an oxygen flow is used to burn the humins deposited on the surface of the catalysts. Derivative thermogravimetric (DTG) graphs are obtained from the first derivative of the TGA results with respect to time or temperature.

3. Results and discussion

3.1 Characterization of fresh catalysts

3.1.1 BET. The textural properties of the catalyst play an important role in the catalytic dehydration of sugars.⁶¹ The BET surface area and pore size distribution of both niobium- and Amberlyst-based heterogeneous solid acid catalysts were measured, and these values are presented in Table 1. As shown in Table 1, both commercially available NbP and NbA exhibit a high BET surface area compared with synthetic NbS-syn and NbP-syn catalysts. However, the average pore diameter of these catalysts is nearly the same. Although the Amb. 15 and Amb. 16 catalysts display lower BET surface area values compared with niobium-based catalysts, they have larger pores.

3.1.2 XRD. Furthermore, XRD is used to characterize the crystalline structure of these catalyst materials. No diffraction peaks are observed in the XRD pattern, suggesting that all fresh catalysts used in this work are amorphous; this finding is compatible with those in previous studies.^{36,62,63}

3.1.3 NH₃-TPD. The acidity of catalyst plays a key role in the catalytic dehydration of fructose to 5-HMF.⁶⁴ In this study, the acidity of niobium based solid acid catalysts was measured by TPD-NH₃ (Fig. 2). However, the Amb-15 and Amb. 36 catalysts decompose under NH₃-TPD conditions, which results in inaccurate results and hence we did not perform the TPD-NH₃ analysis for these.⁶⁵ The decomposition of Amb. 15 and Amb. 36 catalysts at higher temperatures is confirmed by TGA analysis, which will be discussed in Section 3.1.5. The ammonia desorption profile of the catalysts can be divided into three regions: weak ($200\text{--}350 \text{ }^\circ\text{C}$), intermediate or medium ($350\text{--}450 \text{ }^\circ\text{C}$), and strong ($450\text{--}700 \text{ }^\circ\text{C}$) acid sites. As shown in Fig. 2, all catalysts show these three types of acid sites; however, differences between peak intensities exist. The commercial NbP catalyst shows a broad distribution of acid sites and exhibits a high-intensity peak from low temperature

Table 1 Physicochemical properties of different niobium- and Amberlyst-based catalysts

Catalyst	BET surface area ($\text{m}^2 \text{ g}^{-1}$)	Average pore diameter (nm)	B/L ratio	Total acidity (mmol g^{-1})
NbA	155	4	0.24	0.88
NbS-syn	108	5	0.24	0.86
NbP-syn	101	5	0.78	1.01
NbP	246	5	0.70	2.09
Amb. 15	51	29	N/A	—
Amb. 36	30	22	N/A	—

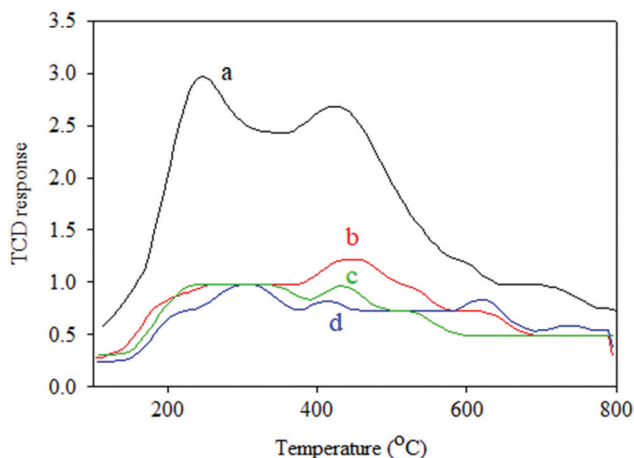


Fig. 2 The TPD-NH₃ profile for fresh NbP (a), NbP-syn (b), NbA (c) and NbS-syn (d).

through to the high-temperature region compared with a similar catalyst prepared by the phosphorylation of niobic acid (NbP-syn). On the other hand, NbA and NbS-syn catalysts exhibit similar intensity peaks, except that one extra shoulder peak appears in the high-temperature region in the NbS-syn catalyst. However, the intensities of these peaks are low compared with the NbP catalyst. The total acidities of all these catalysts are calculated, and these values are presented in Table 1. The total acidity of the NbP catalyst (2.09 mmol g^{-1}) is much higher than those of NbP-syn (1.01 mmol g^{-1}), NbA (0.88 mmol g^{-1}) and

NbS-syn (0.86 mmol g^{-1}) catalysts, and hence the NbP catalyst exhibits more acidity/activity per unit mass in comparison with the others.

3.1.4 Pyridine FT-IR. Furthermore, these catalysts were characterized by pyridine FT-IR analysis to distinguish the nature of the acid sites on the catalyst surface. The FT-IR spectra of the saturated pyridine samples are shown in Fig. 3. All niobium-based catalysts display three different types of pyridine FT-IR peaks. The first peak at 1445 cm^{-1} characterizes the Lewis acid sites, and the second peak at 1540 cm^{-1} is allocated to the Brønsted acid sites. The third pyridine FT-IR peak appears at 1495 cm^{-1} , and this peak characterizes the presence of both Brønsted and Lewis acid sites on the catalyst surface.⁶⁶ The B/L ratio is calculated based on the intensity of the Brønsted and Lewis acid site peaks at 1540 and 1445 cm^{-1} in the pyridine FT-IR spectra, and these values are presented in Table 1. The B/L ratio of these catalysts are in the sequence of NbP-syn > NbP > NbA = NbS-syn. However, the Amberlyst catalysts show only two peaks at 1540 and 1495 cm^{-1} , corresponding to pure Brønsted acid sites. No peak was detected at 1445 cm^{-1} relating to the Lewis acid sites, indicating that the Amberlyst catalysts do not have pure Lewis acid sites.⁶⁷

3.1.5 TGA/DTG. The thermal stabilities of both niobium- and Amberlyst-based catalysts were characterized by TGA/DTG analysis, and the experimental results are shown in Fig. 4 and 5. Fig. 4 shows that the Amb. 15 catalyst exhibits a slightly larger total mass loss (66%), compared with Amb. 36 (61%). The mass loss of the Amberlyst samples consists of two steps for Amb. 36

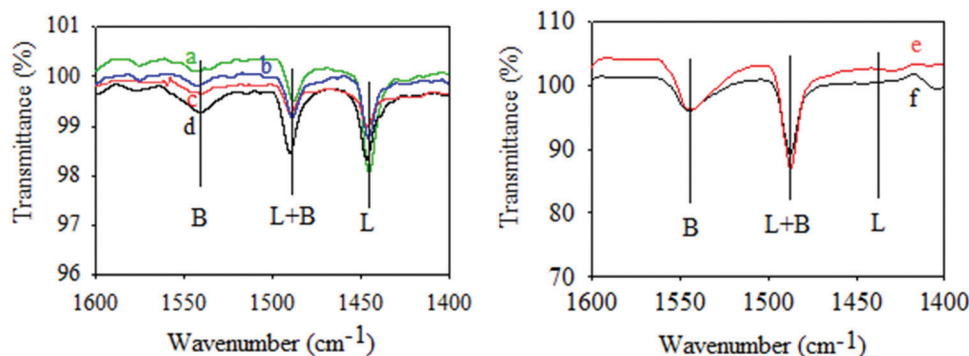


Fig. 3 Py-FTIR spectra of fresh NbA (a), NbS-syn (b), NbP-syn (c), NbP (d), Amb. 36 (e) and Amb. 15 (f).

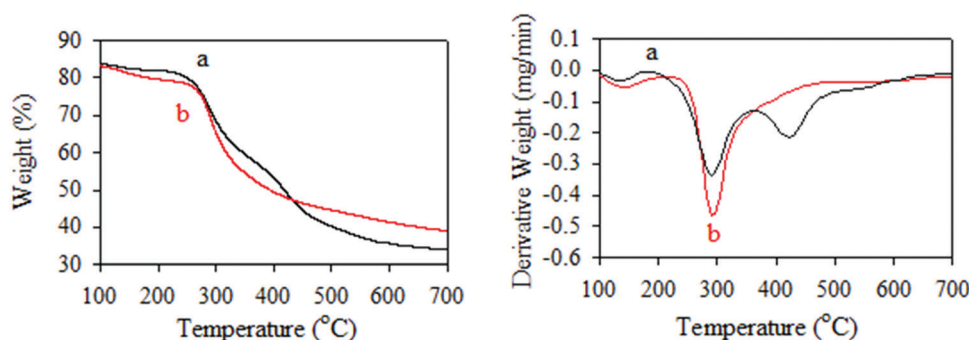


Fig. 4 TGA/DTG graphs for fresh Amberlyst 15 (a) and Amberlyst 36 (b).

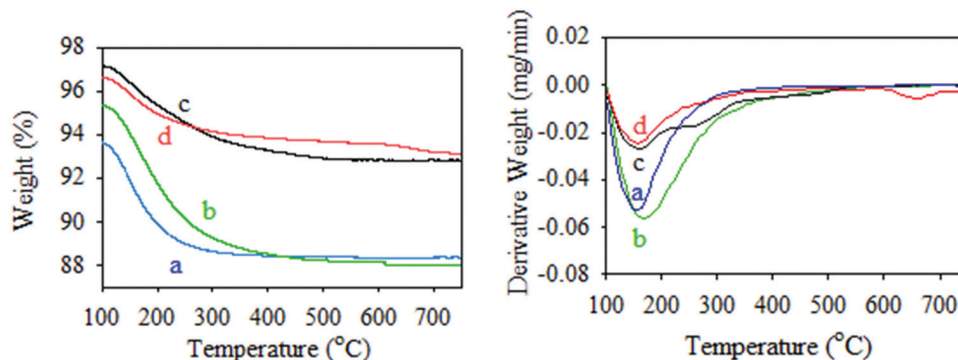


Fig. 5 TGA/DTG graphs for the NbA (a), NbP (b), NbP-syn (c) and NbS-syn (d).

and three steps for Amb. 15, which can be verified by the DTG curves of these two samples. A small peak can be found in the DTG of both Amberlyst catalysts at temperatures up to 200 °C, which is likely associated with the removal of physically adsorbed water. The second mass loss peak in the range of 200–350 °C may be due to the depolymerization of polystyrene chains and decomposition of sulfonic groups. The mass loss peak above 350 °C, which is only seen in Amb. 15, can be attributed to the breakdown of the polymer backbone and the degradation of divinylbenzene.⁶⁸

On the other hand, among the TGA curves of niobium-based catalysts, NbP has the largest total mass loss (12.1%) compared with NbA (11.6%), NbP-syn (7.1%) and NbS-syn (6.7%) (Fig. 5). Whereas a single mass loss peak is found within the temperature range of 100–200 °C in the DTG analysis of all niobium catalysts, indicating the removal of water molecules coordinated to niobium atoms.^{69,70}

3.1.6 FT-IR. Additionally, FT-IR analysis identified different functional groups in the catalyst samples, and the results are presented in Fig. 6. All niobium-based catalysts show a broad O–H band absorption centred at 3400 cm^{-1} and a weak O–H band at 1620 cm^{-1} , which can be assigned to the absorption of water. The commercial NbP and NbP-Syn catalysts have stretching vibrations at around 1000 cm^{-1} that can be attributed to the stretching vibration of the Nb–O–P bond.⁷¹ As expected, this band is absent in NbA and NbS-syn catalysts. Furthermore, the intensity of this peak is greater in NbP, suggesting a higher P content in this catalyst.⁶³ The Amberlyst catalysts have a broad absorption centred at 3440 cm^{-1} because of the overlapping of O–H stretching vibration of water molecules and the N–H stretch of amines. The FT-IR absorption band at around 1700 cm^{-1} represents the C=O stretching vibration. The asymmetric vibration of the C–O–C aliphatic ether and the stretching vibration of the $-\text{CH}_2\text{OH}$ groups can be observed at 1120 cm^{-1} and 1020 cm^{-1} , respectively.⁷² The FT-IR peaks observed between 670 cm^{-1} and 830 cm^{-1} are ascribed to the out-of-plane bending vibration of C–H.

3.2 Continuous flow catalytic dehydration of fructose to 5-HMF

3.2.1 Effects of feeding flow rate and temperature in a single aqueous phase. The continuous-flow selective dehydration of fructose is first performed in a pure water solvent in the presence of the NbA catalyst (18 g catalyst loading). Table S1 (ESI[†]) shows

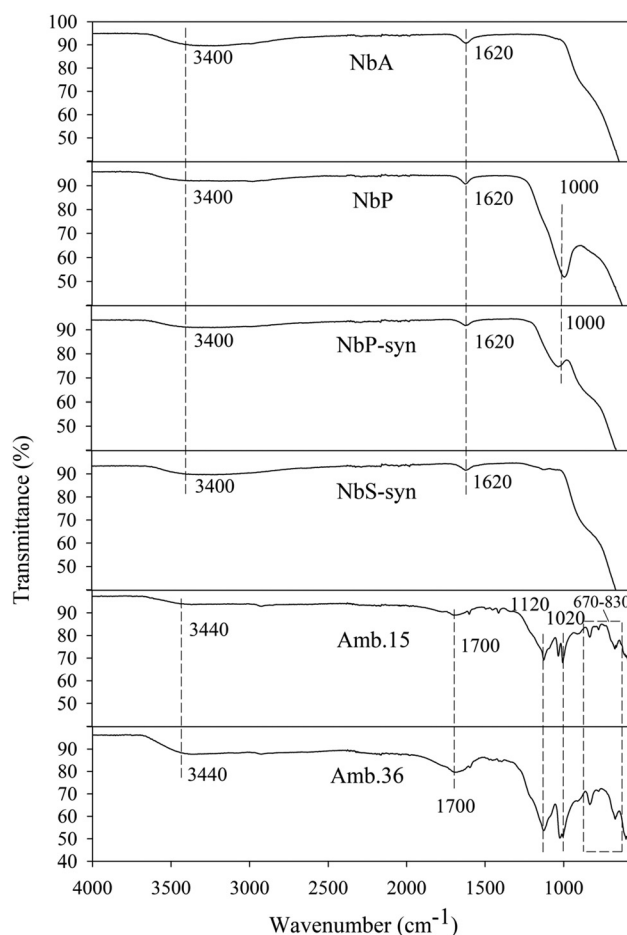


Fig. 6 FT-IR spectra of fresh catalysts.

the effects of the feeding flow rate and temperature on the fructose conversion, 5-HMF selectivity and yield in a single aqueous phase reaction medium. It shows very low 5-HMF yields in the pure water solvent at both feeding flow rates because of the formation of byproducts (as indicated by the high conversion but low selectivity/yield). The main secondary reactions in aqueous media are the rehydration of 5-HMF to levulinic and formic acids and the polymerization of fructose and/or 5-HMF to humins.⁷³ With a constant flow rate (*i.e.*, fixed WHSV), increasing the temperature from 80 °C to 120 °C increases the conversion,

selectivity, and yield of fructose. At a fixed reaction temperature, both fructose conversion and the 5-HMF yield are slightly enhanced by decreasing the flow rate from 1.0 to 0.5 ml min⁻¹ (or reducing the WHSV from 0.333 h⁻¹ to 0.166 h⁻¹). This is due to the increased residence time for fructose inside the reactor. It has been reported that fructose dehydration increases with increasing reaction temperature and residence time.^{26,74} Thus, higher reaction temperatures (>100 °C) and lower feed flow rates (<1.0 ml min⁻¹) are further investigated in the rest of the study.

3.2.2 Effects of feeding flow rate and temperature in a biphasic reaction medium. The performance of the biphasic medium on fructose dehydration is studied with MIBK as the extracting organic phase in the presence of the NbA catalyst (18 g catalyst loading, the same as the reference tests in the single aqueous phase as discussed above). The results are presented in Table S2 (ESI[†]). First, the MIBK solvent flow rate is adjusted at 1.0 ml min⁻¹, while the aqueous feedstock flow rate is tested at 0.5 ml min⁻¹ (*i.e.*, an aqueous-to-organic phase ratio of 1:2 (v/v) containing 100 mg ml⁻¹ fructose and 100 mg ml⁻¹ NaCl. Comparing the experimental results at 120 °C and the 0.5 ml min⁻¹ feeding flow rate (WHSV = 0.166 h⁻¹) from Tables S1 and S2 (ESI[†]) shows that the fructose conversion and 5-HMF yield in the biphasic system are all higher than those in the single aqueous phase. The fructose conversion and 5-HMF yield further increase with an increase in the reaction temperature to 130 °C, and other reaction conditions are kept the same (0.5 ml min⁻¹ of aqueous feeding flow rate containing 100 mg ml⁻¹ fructose and 100 mg ml⁻¹ NaCl, and an aqueous-to-organic phase ratio of 1:2 (v/v)). Therefore, these results demonstrate the promoting effects of MIBK as an extracting organic solvent on the conversion of fructose to 5-HMF. It has been widely believed that the presence of an organic solvent can promote the dehydration reaction by extracting the 5-HMF into the organic phase immediately and suppressing the unwanted side reactions.^{26,75}

The effects of the biphasic reaction medium are further studied at 130 °C and decreasing the aqueous-to-organic phase ratio (A/O) to 1:5 (v/v) through reducing the aqueous feeding flow rate to 0.25 ml min⁻¹ and increasing the MIBK flow rate to 1.25 ml min⁻¹. The fructose and NaCl concentrations in the aqueous feed are also increased to 400 and 200 mg ml⁻¹, respectively. The results presented in Table S2 (ESI[†]) show that using more extracting organic solvent (decreasing the A/O ratio), more phase transfer catalyst, and a more concentrated feedstock has a positive effect on the fructose dehydration reaction, resulting in a significantly increased 5-HMF yield (23%), although a lower fructose conversion (64.8%) is observed likely due to the decreased retention time (with a higher WHSV = 0.333 h⁻¹). For economic considerations, the feedstock solution should be as concentrated as possible. However, in practice, a concentrated feedstock solution might lower the 5-HMF selectivity because of a higher rate of cross-polymerization and formation of humins.^{19,73} For instance, Fan *et al.* observed an initial rise followed by a drop in 5-HMF selectivity when the initial fructose concentration was increased from 10 wt% to 30 wt% and then to 50 wt%, where a continuous drop in conversion was observed when

increasing the feed concentration from 10 wt% to 30 wt% and then to 50 wt%.²⁶

The residence time of the reaction feed in the catalytic bed can be estimated by the reciprocal of the WHSV. A longer retention time has a positive effect on fructose dehydration to 5-HMF; however, overly long retention times might also cause the decomposition of 5-HMF to other by-products, subsequently decreasing the 5-HMF selectivity and yield.^{28,76} In the abovementioned experiments at 130 °C, the feedstock concentration is increased four times (from 100 mg ml⁻¹ to 400 mg ml⁻¹), and the aqueous feeding flow rate is reduced to half of the initial flow (from 0.50 ml min⁻¹ to 0.25 ml min⁻¹). The fructose conversion decreases from 93.5 to 64.8%, while the 5-HMF selectivity and yield change to 35% and 23%, respectively. Other researchers have reported similar observations during the catalytic dehydration of fructose to 5-HMF over different solid acid catalysts.^{21,22} It should be noted that using more extracting organic solvent by decreasing the A/O ratio from 1:2 to 1:5 (v/v) and using a higher concentration of phase transfer catalyst (NaCl) could also enhance the 5-HMF selectivity and yield by suppressing the side reactions (*e.g.*, polymerization and rehydration of 5-HMF) and the formation of humins.^{24,50,77}

Based on the preceding experimental results, a high fructose feedstock solution (400 mg ml⁻¹ or ~40 wt%) and an A/O of 1:5 (v/v) (a feeding flow rate of 0.25 ml min⁻¹ and an MIBK flow rate of 1.25 ml min⁻¹) are used for the rest of the study, unless stated otherwise.

3.2.3 Catalytic performance of different solid acid catalysts for continuous dehydration of fructose to 5-HMF. Based on the results of the NbA catalyst, we compare various heterogeneous solid acid catalysts, including NbA, NbS-syn, NbP-syn, NbP, Amb. 15 and Amb. 36, for selective dehydration of fructose to 5-HMF at 130 °C under the above experimental reaction conditions, except for Amb. 15 (tested at 110 °C since the maximum recommended operating temperature for this catalyst is 110 °C). The catalytic results are presented in Table 2.

As shown in Table 2, both NbP and NbP-syn catalysts exhibit a high fructose conversion (79–91%) and 5-HMF yield (34%), whereas the NbA and NbS-syn catalysts produce only 63–64% fructose conversion and 22% 5-HMF yield, respectively. It was mentioned that under all the experimental reaction conditions

Table 2 Performance of different solid catalysts in fructose dehydration at 130 °C^a

Catalyst	Fructose conversion (%)	5-HMF selectivity (%)	5-HMF yield (%)
NbA	64.8 ± 0.8	34.8 ± 2.1	22.6 ± 2.8
NbS-syn	63.4 ± 1.1	35.0 ± 1.4	22.2 ± 1.9
NbP-syn	79.8 ± 1.2	43.5 ± 0.5	34.7 ± 1.3
NbP	91.8 ± 1.5	37.6 ± 0.6	34.5 ± 1.6
Amb. 15 ^b	35.1 ± 0.4	4.9 ± 1.8	1.7 ± 2.5
Amb. 36	40.2 ± 1.0	10.1 ± 1.6	4.2 ± 2.6

^a Initial fructose concentration 400 mg ml⁻¹ (~40 wt%), NaCl concentration 200 mg ml⁻¹, feeding flow rate 0.25 ml min⁻¹, MIBK flow rate 1.25 ml min⁻¹, A/O = 1:5 (v/v). ^b The operating temperature for this catalyst is 110 °C.

over these catalysts, no levulinic acid and formic acid were detected in the product mixture. The superior catalytic activity of the niobium phosphate catalyst compared with niobic acid has also been reported by Carniti *et al.* for the dehydration of fructose to 5-HMF in an aqueous medium.⁷⁴ This could be related to the effective acidity in terms of the total number of acid sites as well as the nature of the acid sites (the ratio of Brønsted to Lewis acid sites [B/L]) on the catalyst surface. As seen in Table 1, the total number of acid sites on both NbP (2.09 mmol g⁻¹) and NbP-syn (1.01 mmol g⁻¹) catalysts is much higher than that of both NbA and NbS-syn (0.86–0.88 mmol g⁻¹) catalysts. In addition, they also exhibit higher B/L ratios (0.70–0.78) than NbA and NbS-syn (0.24). It is well known that the presence of both Lewis and Brønsted acid sites should be responsible for catalyzing the dehydration of carbohydrates. Weingarten *et al.* studied the dehydration of xylose over solid acids, where the furfural selectivity was reported to depend on the nature of the acid sites on the catalyst surface. Brønsted acid sites were shown to be more selective towards furfural production than Lewis acid sites.⁷⁸

In this study, both NbP and NbP-syn catalysts show almost the same activity in terms of producing the same quantity of 5-HMF, which can be attributed to the high B/L ratio of these catalysts compared with the other catalysts examined in this work. However, the fructose conversion is higher in the presence of the NbP catalyst. This might be due to its high BET surface area (246 m² g⁻¹); in addition, more total acid sites (2.09 mmol g⁻¹) are available on the catalyst surface than those of any other catalysts being examined. On the other hand, both Amb. 15 and Amb. 36 catalysts give very low fructose conversions (35–40%) and poor 5-HMF yields (2–4%) under the above-stated reaction conditions.

3.2.4 Effects of reaction temperature. The reaction temperature plays a major role in the selective synthesis of 5-HMF from carbohydrates. In this study, the effects of reaction temperature (ranging from 110 to 150 °C) on the selective dehydration of fructose to 5-HMF over three different catalysts (NbP, NbS-syn and Amb. 36) were examined under the following reaction conditions: a feed flow rate of 0.25 ml min⁻¹ (WHSV = 0.428 h⁻¹), an initial fructose concentration of 400 mg ml⁻¹ (~40 wt%), NaCl concentration of 200 mg ml⁻¹, and A/O = 1:5 (v/v). The catalytic activity results are shown in Fig. 7.

The results show that all catalysts can improve both fructose conversion and 5-HMF yield by increasing the reaction temperature. As expected, these results agree with those reported by other researchers.^{24,26,74} However, the Amb. 36 catalyst exhibits drastic improvement in both fructose conversion and 5-HMF selectivity upon increasing the reaction temperature from 110 °C to 150 °C. For instance, the fructose conversion increases from 30.3% at 110 °C to 77.5% at 150 °C. Overall, a maximum of 78–99% fructose conversion and 54–57% of 5-HMF yields are obtained at 150 °C for these three catalysts. Especially, the performance of the Amb. 36 is exceptionally good with respect to 5-HMF selectivity, as high as 70.1% was obtained. Despite the slight decrease in fructose conversion obtained with the Amb. 36 catalyst compared with NbP and

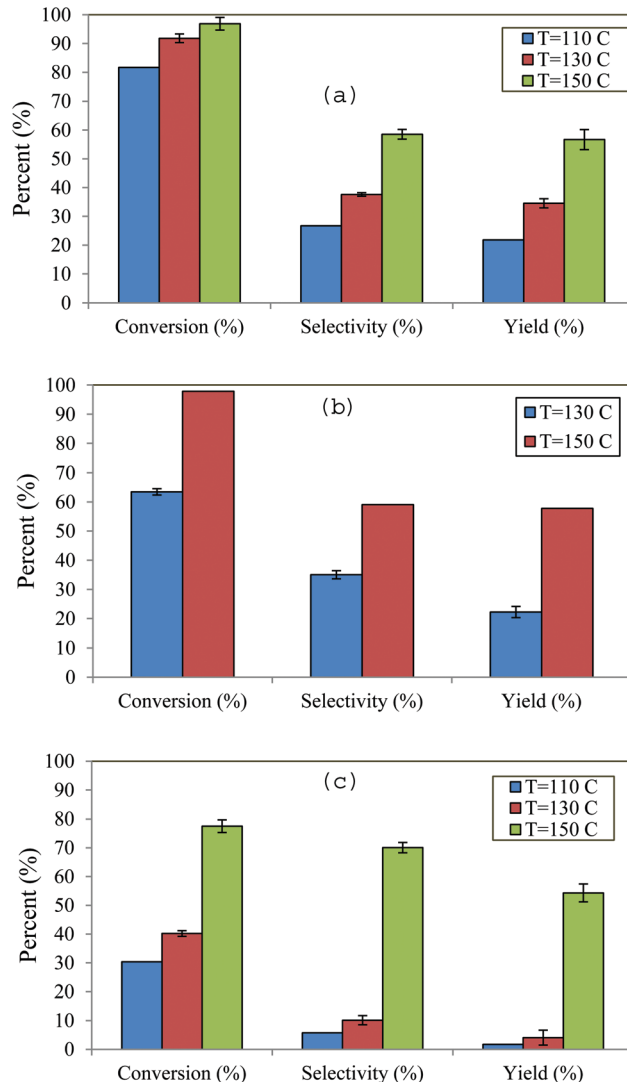


Fig. 7 Effects of reaction temperature on the activity of NbP (a), NbS-syn (b) and Amb. 36 (c). (feeding flow rate 0.25 ml min⁻¹ (WHSV = 0.428 h⁻¹), initial fructose concentration 400 mg ml⁻¹ (~40 wt%), NaCl concentration 200 mg ml⁻¹, and A/O = 1:5 (v/v).)

NbS-syn catalysts, the 5-HMF yields for these catalysts are nearly equal. Therefore, from economic point of view, the Amb. 36 catalyst is more favourable than the NbP and NbS-syn catalysts for the dehydration of fructose to 5-HMF.

3.2.5 Effects of NaCl on 5-HMF selectivity. Many studies have shown that the addition of NaCl to the biphasic reaction medium (H₂O/MIBK) improves the 5-HMF selectivity.^{30,79} The reason is that addition of NaCl to the reaction medium modifies the ionic strength of water, which improves the partitioning of 5-HMF into MIBK. In this study, we also examine the presence and the absence of NaCl in the feedstock solution for the continuous synthesis of 5-HMF over the NbP catalyst at two different reaction temperatures (130 °C and 150 °C) under the following reaction conditions: 400 mg ml⁻¹ fructose concentration, 0.25 ml min⁻¹ feed flow rate (WHSV = 0.428 h⁻¹), and A/O of 1:5 (v/v).

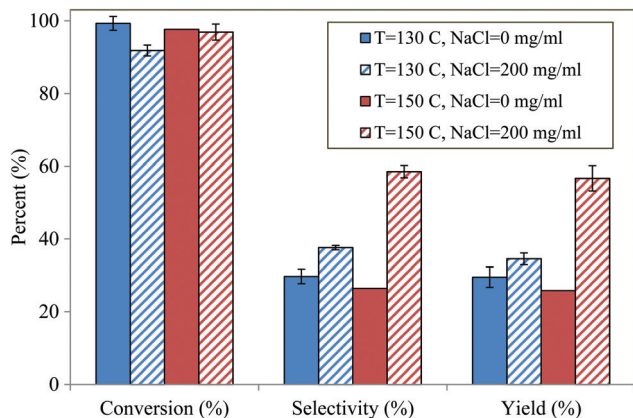


Fig. 8 Effects of NaCl on the activity of the NbP catalyst at 130 °C and 150 °C (feeding flow rate 0.25 ml min⁻¹ (WHSV = 0.428 h⁻¹), initial fructose concentration 400 mg ml⁻¹ (~40 wt%), A/O = 1:5 (v/v)).

As shown in Fig. 8, the fructose conversion with and without phase transfer catalyst remains almost constant (>90%). However, both 5-HMF selectivity and yield increased when NaCl is present in the aqueous feedstock solution, and this increase becomes more evident at a higher reaction temperature (150 °C). These results demonstrate that the presence of NaCl in the aqueous feed contribute to the *in situ* extraction of 5-HMF from the aqueous phase to the organic phase, which then suppresses the side reactions and hence increases the 5-HMF selectivity and yield. With the NbP catalyst and 200 mg ml⁻¹ NaCl, fructose dehydration achieves the highest selectivity of 58.5% and yield of 56.7% at 150 °C.

3.2.6 Effects of catalyst loading and initial fructose concentration. Previous studies have shown that increasing the catalyst dosage could result in a higher conversion because of the increase in residence time and catalyst active sites.²² However, it can also result in reduced 5-HMF selectivity and yield due to the longer residence time that favors the side reactions, for example, rehydration and polymerization of 5-HMF and intermediates into levulinic acid and other by-products.^{26,28} In our experiments, the effects of catalyst loading and initial fructose concentration on the feedstock conversion and product selectivity are studied by changing the amount of NbP and Amb. 36 catalysts and varying the initial fructose concentration in the aqueous feedstock solution. The results for the NbP catalyst are presented in Table 3. No significant change in the catalytic results is observed when the catalyst amount is reduced from 14 g to 7 g

Table 3 Effects of catalyst loading and initial fructose concentration on the activity of NbP at 150 °C^a

Catalyst loading (g)	14 g	7 g	7 g
Fructose concentration (mg ml ⁻¹)	400 ^b	400 ^c	200 ^b
Conversion (%)	96.9 ± 2.2	98.9 ± 1.9	99.7 ± 1.6
Selectivity (%)	58.5 ± 1.7	54.9 ± 3.1	45.1 ± 0.9
Yield (%)	56.7 ± 3.5	54.3 ± 3.5	44.9 ± 1.8

^a Feeding flow rate 0.25 ml min⁻¹, NaCl concentration 200 mg ml⁻¹, A/O = 1:5 (v/v), 150 °C. ^b WHSV = 0.428 h⁻¹. ^c WHSV = 0.856 h⁻¹.

by using 400 mg ml⁻¹ of initial fructose concentration (while the WHSV is doubled or the residence time is reduced to half). This signifies that there are sufficient catalytic sites for the conversion of fructose even at a low catalyst dosage of 7 g. However, a high catalyst dosage of 14 g does not show any detrimental effects on the product selectivity and yield. Although with a fixed amount of catalyst (7 g) and the initial fructose concentration in the aqueous feedstock solution being reduced from 400 mg ml⁻¹ to 200 mg ml⁻¹ (*i.e.*, reducing the WHSV to half or doubling the residence time), this favors the side reaction leading to the 5-HMF yield dropping from 55% to 45%.

On the other hand, with a fixed amount of Amb. 36 catalyst (14 g) and reducing the initial fructose concentration from 400 mg ml⁻¹ to 200 mg ml⁻¹ *via* the feeding flow rate (*i.e.*, reducing the WHSV to half or doubling the residence time) even though the conversion of fructose is more or less the same, the 5-HMF yield is significantly decreased from 54% to 33% (Table 4). At a fixed fructose concentration (200 mg ml⁻¹), when the catalyst loading is increased from 14 g to 24 g (*i.e.*, reducing the WHSV by around 40% or increasing the residence time by around 40%), the fructose conversion increases from 73.6 to 91.9%, while the 5-HMF yield drastically increases from 33% to 60%. Therefore, for Amb. 36, simply increasing the catalyst loading can effectively enhance the performance of the catalyst in the catalytic dehydration of fructose to 5-HMF.

Based on the preceding results and discussion, NbP, NbS-syn and Amb. 36 are the most active catalysts among all catalysts tested in this work, and the optimal conditions for the catalytic dehydration of fructose to 5-HMF in the continuous-flow reactor are summarized as follows: a temperature of 150 °C, aqueous feed flow rate 0.25 ml min⁻¹, organic (MIBK) flow rate 1.25 ml min⁻¹, fructose concentration in the aqueous feedstock solution 200 or 400 mg ml⁻¹, and NaCl concentration in the aqueous feedstock solution 200 mg ml⁻¹. Table 5 summarizes the activity of the three catalysts under the optimal conditions for the production of 5-HMF from fructose in the continuous-flow reactor. With these three catalysts (NbP, NbS-syn and Amb. 36) under the optimal conditions, fructose dehydration in the continuous-flow reactor produces 5-HMF with both high selectivity (55–70%) and high yield (54–60%).

3.2.7 Catalyst reusability study. The possibility of reusing and recycling the catalysts was studied by testing the used Amb. 36 and NbS-syn under the optimal conditions. After running the experiments for 8 hours on stream, the system is cooled

Table 4 Effects of catalyst loading and initial fructose concentration on activity of Amb. 36 at 150 °C^a

Catalyst loading (g)	14 g	24 g	24 g
Fructose concentration (mg ml ⁻¹)	400 ^b	200 ^c	200 ^d
Conversion (%)	77.5 ± 2.2	73.6 ± 1.5	91.9 ± 0.8
Selectivity (%)	70.1 ± 1.8	44.5 ± 2.7	64.8 ± 1.7
Yield (%)	54.3 ± 3.1	32.8 ± 3.3	59.6 ± 1.9

^a Feeding flow rate 0.25 ml min⁻¹, NaCl concentration 200 mg ml⁻¹, A/O = 1:5 (v/v). ^b WHSV = 0.428 h⁻¹. ^c WHSV = 0.214 h⁻¹. ^d WHSV = 0.125 h⁻¹.

Table 5 Catalytic activity of NbP, NbS-syn and Amb. 36 under optimal conditions for the production of 5-HMF from fructose in a continuous-flow reactor

	NbP		NbS-syn	Amb. 36	
Catalyst loading (g)	7	14	14	14	24
Fructose concentration (mg ml ⁻¹)	400 ^a	400 ^b	400 ^b	400 ^b	200 ^c
Conversion (%)	98.9 ± 1.9	96.9 ± 2.2	97.8	77.5 ± 2.2	91.9 ± 0.8
Selectivity (%)	54.9 ± 3.1	58.5 ± 1.7	59.1	70.1 ± 1.8	64.8 ± 1.7
Yield (%)	54.3 ± 3.5	56.7 ± 3.5	57.8	54.3 ± 3.1	59.6 ± 1.9

^a WHSV = 0.856 h⁻¹. ^b WHSV = 0.428 h⁻¹. ^c WHSV = 0.125 h⁻¹.

down and washed by pumping distilled water through the reactor with the used catalysts packed inside. Left overnight, the reactor is tested for another 8 hours on stream again with fresh feedstock and the used catalyst left inside the reactor, and the results are compared with those achieved with the fresh

Table 6 Performance of NbS-syn and Amb. 36 used catalysts at 150 °C^a

	NbS-syn ^b		Amb. 36 ^c	
	Fresh catalyst	Used catalyst	Fresh catalyst	Used catalyst
Conversion (%)	97.8	87.7 ± 2.1	91.9 ± 0.8	81.7 ± 2.2
Selectivity (%)	59.1	36.7 ± 1.8	64.8 ± 1.7	66.3 ± 0.8
Yield (%)	57.8	32.2 ± 2.9	59.6 ± 1.9	54.2 ± 2.5

^a Feeding flow rate 0.25 ml min⁻¹, NaCl concentration 200 mg ml⁻¹, A/O = 1:5 (v/v). ^b Catalyst dosage 14 g, initial fructose concentration 400 mg ml⁻¹ (WHSV = 0.428 h⁻¹). ^c Catalyst dosage 24 g, initial fructose concentration 200 mg ml⁻¹ (WHSV = 0.125 h⁻¹).

catalysts (see Table 6). The catalytic activity of the used NbS-syn is reduced compared with the fresh catalyst, resulting in a lower fructose conversion as well as a decreased selectivity and yield. This is likely due to the deposition of humins or other organic residues on the catalyst surface, which hinders access to the catalytic active sites. In contrast, the Amb. 36 catalyst shows a superb stability after 8 hours of on-stream analysis, with an even greater selectivity and only a slight decrease in fructose conversion and 5-HMF yield. Therefore, Amb. 36 is expected to have a longer lifetime in real applications.

3.2.8 Reaction mechanism. Based on the experimental results and the characteristic properties of the catalyst, a plausible reaction mechanism for the dehydration of fructose to 5-HMF over a highly active and selective NbP or Amb. 36 catalyst is proposed as follows. Generally, the conversion of fructose to 5-HMF should require Brønsted acid sites.^{3,80} The pyridine FT-IR results show that both NbP and Amb. 36 catalysts contain Brønsted acid sites on the catalyst surface and these are strong enough to produce 5-HMF from fructose. Fig. 9 shows the dehydration mechanism of fructose to 5-HMF over NbP or Amb. 36 catalysts. Fructose can exist in the cyclic furanose structure, which undergoes three consecutive dehydration reactions with the aid of Brønsted acid sites on the catalyst surface, leading to the formation of 5-HMF. However, the experimental results show that the 5-HMF selectivity over the NbP catalyst is slightly lower than for Amb. 36. This might be due to the Lewis acid sites on the NbP catalyst that can initiate secondary reactions between the formed 5-HMF and the unreacted sugar or self-polymerization of 5-HMF to produce a polymeric product called humins. Humin deposition is observed over the spent NbP catalyst. Experimental results show that fructose conversion on the niobium catalysts is significantly higher than for the Brønsted acid-based Amb. 36 catalyst.

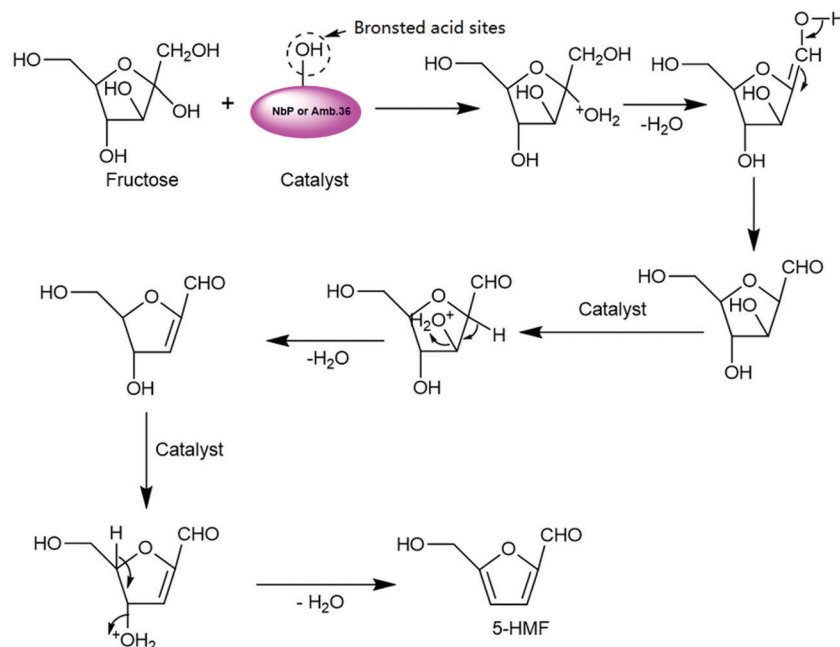


Fig. 9 Proposed reaction mechanism for the selective dehydration of fructose to 5-HMF.

The Lewis acidity on the niobium-based catalysts certainly helps to increase the fructose conversion but decreases the 5-HMF selectivity slightly. No formation of levulinic acid or formic acid is detected in the HPLC analysis of the reaction mixture, which indicates the absence of rehydration of 5-HMF over these catalysts under the present experimental conditions.

4. Conclusions

In summary, the continuous synthesis of 5-HMF from fructose was investigated in a biphasic continuous-flow tubular reactor using different solid acid catalysts including niobium phosphate (NbP), niobic acid (NbA), phosphated niobia (NbP-syn), sulfated niobia (NbS-syn), Amberlyst 15 (Amb. 15) and Amberlyst 36 (Amb. 36). Among these catalysts, Amb. 36, NbP and NbP-syn exhibit superior catalytic activity and selectivity. Various reaction parameters such as the effects of the initial fructose concentration, catalyst loading, reaction temperature, aqueous-to-organic solvent flow ratio, phase transfer catalyst and the feed flow rate were investigated to obtain a high fructose conversion and 5-HMF yield. Under the optimal conditions of 150 °C, 0.25 ml min⁻¹ aqueous feed flow, 1.25 ml min⁻¹ organic (MIBK) solvent flow, 200 or 400 mg ml⁻¹ fructose feed flow and 200 mg ml⁻¹ of NaCl in the aqueous feedstock solution, 78–99% fructose conversion, and 54–60% 5-HMF yield were obtained over the three different solid acid catalysts (NbP, NbP-syn and Amb. 36). Moreover, NbP and NbP-syn catalysts showed considerably high catalytic activity and selectivity even at lower reaction temperatures (110 °C and 130 °C) compared with the other catalysts being studied, which could be attributed to the high acidity and high B/L ratio. In addition, the Amb. 36 catalyst showed superb stability even after an 8 h period of on stream analysis, with better 5-HMF selectivity and only a slight decrease in fructose conversion and 5-HMF yield. Therefore, Amb. 36 is expected to have a longer lifetime in real applications.

Conflicts of interest

There are no conflicts to declare.

Acknowledgements

The authors acknowledge the financial support from NSERC Discovery Program, Ontario government via the NSERC/FPINnovations Industrial Research Chair Program and the ORF-RE Program in Forest Biorefinery.

References

- 1 D. M. Alonso, S. G. Wettstein and J. A. Dumesic, *Chem. Soc. Rev.*, 2012, **41**, 8075–8098.
- 2 C. H. Zhou, X. Xia, C. X. Lin, D. S. Tong and J. Beltramini, *Chem. Soc. Rev.*, 2011, **40**, 5588–5617.
- 3 B. Saha and M. M. Abu-omar, *Green Chem.*, 2014, **16**, 24–38.
- 4 P. Pal and S. Saravanamurugan, *ChemSusChem*, 2019, **12**, 145–163.
- 5 Z. Xu, P. Yan, K. Liu, L. Wan, W. Xu, H. Li, X. Liu and Z. C. Zhang, *ChemSusChem*, 2016, **9**, 1255–1258.
- 6 A. García-Ortiz, J. D. Vidal, M. J. Climent, P. Concepción, A. Corma and S. Iborra, *ACS Sustainable Chem. Eng.*, 2019, **7**, 6243–6250.
- 7 J. N. Chheda and J. A. Dumesic, *Catal. Today*, 2007, **123**, 59–70.
- 8 C. J. Barrett, J. N. Chheda, G. W. Huber and J. A. Dumesic, *Appl. Catal., B*, 2006, **66**, 111–118.
- 9 L. Hu, J. Xu, S. Zhou, A. He, X. Tang, L. Lin, J. Xu and Y. Zhao, *ACS Catal.*, 2018, **8**, 2959–2980.
- 10 L. Hu, L. Lin, Z. Wu, S. Zhou and S. Liu, *Renewable Sustainable Energy Rev.*, 2017, 230–257.
- 11 K. T. V. Rao, J. L. Rogers, S. Souzanchi, L. Dessbesell, M. B. Ray and C. (Charles) Xu, *ChemSusChem*, 2018, **11**, 3323–3334.
- 12 J. Zhang, J. Li, Y. Tang, L. Lin and M. Long, *Carbohydr. Polym.*, 2015, 420–428.
- 13 K. T. V. Rao, Y. Hu, Z. Yuan, Y. Zhang and C. (Charles) Xu, *Chem. Eng. J.*, 2021, **404**, 127063.
- 14 A. J. J. E. Eerhart, A. P. C. Faaij and M. K. Patel, *Energy Environ. Sci.*, 2012, **5**, 6407–6422.
- 15 R. J. I. Knoop, W. Vogelzang, J. Van Haveren and D. S. Van Es, *J. Polym. Sci., Part A: Polym. Chem.*, 2013, **51**, 4191–4199.
- 16 Z. Yuan, Y. Zhang and C. Xu, *RSC Adv.*, 2014, **4**, 31829–31835.
- 17 Y. Zhang, Z. Yuan and C. Xu, *AIChE J.*, 2015, **61**, 1275–1283.
- 18 A. I. Torres, P. Daoutidis and M. Tsapatsis, *Energy Environ. Sci.*, 2010, **3**, 1560–1572.
- 19 B. F. M. Kuster, *Starch/Staerke*, 1990, **42**, 314–321.
- 20 T. Ståhlberg, M. G. Sørensen and A. Riisager, *Green Chem.*, 2010, **12**, 321–325.
- 21 F. S. Asghari and H. Yoshida, *Carbohydr. Res.*, 2006, **341**, 2379–2387.
- 22 N. Lucas, G. Kokate, A. Nagpure and S. Chilukuri, *Microporous Mesoporous Mater.*, 2013, **181**, 38–46.
- 23 S. Caratzoulas and D. G. Vlachos, *Carbohydr. Res.*, 2011, **346**, 664–672.
- 24 X. Qi, M. Watanabe, T. M. Aida and R. L. Smith Jr, *Green Chem.*, 2009, **11**, 1327–1331.
- 25 G. Raveendra, M. Srinivas, N. Pasha, A. V. Prasada Rao, P. S. Sai Prasad and N. Lingaiah, *React. Kinet., Mech. Catal.*, 2015, **115**, 663–678.
- 26 C. Fan, H. Guan, H. Zhang, J. Wang, S. Wang and X. Wang, *Biomass Bioenergy*, 2011, **35**, 2659–2665.
- 27 P. Carniti, A. Gervasini and M. Marzo, *Catal. Commun.*, 2011, **12**, 1122–1126.
- 28 F. Yang, Q. Liu, X. Bai and Y. Du, *Bioresour. Technol.*, 2011, **102**, 3424–3429.
- 29 R. L. de Souza, H. Yu, F. Rataboul and N. Essayem, *Challenges*, 2012, **3**, 212–232.
- 30 Y. Román-Leshkov and J. a. Dumesic, *Top. Catal.*, 2009, **52**, 297–303.
- 31 J. N. Chheda and J. a. Dumesic, *Science*, 2006, **312**, 1933.
- 32 L. Qi and I. T. Horváth, *ACS Catal.*, 2012, **2**, 2247–2249.
- 33 A. H. Motagamwala, W. Won, C. Sener, D. M. Alonso, C. T. Maravelias and J. A. Dumesic, *Sci. Adv.*, 2018, **4**, 1–9.

- 34 M. T. Reche, A. Osatiashtiani, L. J. Durndell, M. A. Isaacs, Á. Silva, A. F. Lee and K. Wilson, *Catal. Sci. Technol.*, 2016, **6**, 7334–7341.
- 35 N. K. Gupta, A. Fukuoka and K. Nakajima, *ACS Catal.*, 2017, **7**, 2430–2436.
- 36 Y. Zhang, J. Wang, X. Li, X. Liu, Y. Xia, B. Hu, G. Lu and Y. Wang, *Fuel*, 2015, **139**, 301–307.
- 37 C. Carlini, M. Giuttari, A. Maria Raspolli Galletti, G. Sbrana, T. Armaroli and G. Busca, *Appl. Catal., A*, 1999, **183**, 295–302.
- 38 J. Najafi Sarpiri, A. Najafi Chermahini, M. Saraji and A. Shahvar, *Renewable Energy*, 2021, **164**, 11–22.
- 39 N. Lopes da Costa, L. Guedes Pereira, J. V. Mendes Resende, C. A. Diaz Mendoza, K. Kaiser Ferreira, C. Detoni, M. M. V. M. Souza and F. N. D. C. Gomes, *Mol. Catal.*, 2021, **500**, DOI: 10.1016/j.mcat.2020.111334.
- 40 R. Tomer and P. Biswas, *New J. Chem.*, 2020, **44**, 20734–20750.
- 41 Y. Zhou, L. Zhang and S. Tao, *ACS Appl. Nano Mater.*, 2019, **2**, 5125–5131.
- 42 Y. Zhong, Q. Yao, P. Zhang, H. Li, Q. Deng, J. Wang, Z. Zeng and S. Deng, *Ind. Eng. Chem. Res.*, 2020, **59**, 22068–22078.
- 43 G. Delgado Martin, C. E. Bounoukta, F. Ammari, M. I. Domínguez, A. Monzón, S. Ivanova and M. Á. Centeno, *Catal. Today*, 2021, **366**, 68–76.
- 44 X. Jia, I. K. M. Yu, D. C. W. Tsang and A. C. K. Yip, *Microporous Mesoporous Mater.*, 2019, **284**, 43–52.
- 45 S. P. Simeonov, J. A. S. Coelho and C. A. M. Afonso, *ChemSusChem*, 2012, **5**, 1388–1391.
- 46 C. Antonetti, A. M. Raspolli Galletti, S. Fulignati and D. Licursi, *Catal. Commun.*, 2017, **97**, 146–150.
- 47 P. Daorattanachai, S. Namuangruk, N. Viriya-empikul, N. Laosiripojana and K. Faungnawakij, *J. Ind. Eng. Chem.*, 2012, **18**, 1893–1901.
- 48 Y. Román-Leshkov, J. N. Chheda and J. A. Dumesic, *Science*, 2006, **312**, 1933–1937.
- 49 J. Y. G. Chan and Y. Zhang, *ChemSusChem*, 2009, **2**, 731–734.
- 50 B. F. M. Kuster and H. J. C. van der Steen, *Starch/Staerke*, 1977, **29**, 99–103.
- 51 M. Brasholz, K. von Känel, C. H. Hornung, S. Saubern and J. Tsanaktsidis, *Green Chem.*, 2011, **13**, 1114–1117.
- 52 T. M. Aida, Y. Sato, M. Watanabe, K. Tajima, T. Nonaka, H. Hattori and K. Arai, *J. Supercrit. Fluids*, 2007, **40**, 381–388.
- 53 W. Guo, H. J. Heeres and J. Yue, *Chem. Eng. J.*, 2020, **381**, 122754.
- 54 Y. Muranaka, K. Matsubara, T. Maki, S. Asano, H. Nakagawa and K. Mae, *ACS Omega*, 2020, **5**, 9384–9390.
- 55 M. Sayed, N. Warlin, C. Hultheberg, I. Munslow, S. Lundmark, O. Pajalic, P. Tunå, B. Zhang, S.-H. Pyo and R. Hatti-Kaul, *Green Chem.*, 2020, **22**, 5402–5413.
- 56 C. V. McNeff, D. T. Nowlan, L. C. McNeff, B. Yan and R. L. Fedie, *Appl. Catal., A*, 2010, **384**, 65–69.
- 57 C. Zhu, C. Cai, Q. Liu, W. Li, J. Tan, C. Wang, L. Chen, Q. Zhang and L. Ma, *ChemistrySelect*, 2018, **3**, 10983–10990.
- 58 C. Sonsiam, A. Kaewchada, S. Pumrod and A. Jaree, *Chem. Eng. Process.*, 2019, **138**, 65–72.
- 59 M. H. Tucker, A. J. Crisci, B. N. Wigington, N. Phadke, R. Alamillo, J. Zhang, S. L. Scott and J. A. Dumesic, *ACS Catal.*, 2012, **2**, 1865–1876.
- 60 B. Pholjaroen, N. Li, Z. Wang, A. Wang and T. Zhang, *J. Energy Chem.*, 2013, **22**, 826–832.
- 61 K. T. V. Rao, S. Souzanchi, Z. Yuan and C. Xu, *New J. Chem.*, 2019, **43**, 12483–12493.
- 62 D. Prasetyoko, Z. Ramli, S. Endud and H. Nur, *Adv. Mater. Sci. Eng.*, 2008, **2008**, 1–12.
- 63 Y. Zhang, J. Wang, J. Ren, X. Liu, X. Li, Y. Xia, G. Lu and Y. Wang, *Catal. Sci. Technol.*, 2012, **2**, 2485–2491.
- 64 C. Bispo, K. De Oliveira Vigier, M. Sardo, N. Bion, L. Mafra, P. Ferreira and F. Jérôme, *Catal. Sci. Technol.*, 2014, **4**, 2235–2240.
- 65 P. F. Siril, H. E. Cross and D. R. Brown, *J. Mol. Catal. A: Chem.*, 2008, **279**, 63–68.
- 66 V. V. Ordonsky, V. L. Sushkevich, J. C. Schouten, J. Van Der Schaaf and T. A. Nijhuis, *J. Catal.*, 2013, **300**, 37–46.
- 67 B. Ikizer, N. Oktar and T. Dogu, *Fuel Process. Technol.*, 2015, **138**, 570–577.
- 68 G. Fan, C. Liao, T. Fang, S. Luo and G. Song, *Carbohydr. Polym.*, 2014, **112**, 203–209.
- 69 C. C. M. Pereira and E. R. Lachter, *Appl. Catal., A*, 2004, **266**, 67–72.
- 70 M. H. C. de la Cruz, J. F. C. da Silva and E. R. Lachter, *Catal. Today*, 2006, **118**, 379–384.
- 71 K. T. V. Rao, S. Souzanchi, Z. Yuan, M. B. Ray and C. Xu, *RSC Adv.*, 2017, **7**, 48501–48511.
- 72 A. Wolowicz and Z. Hubicki, *Chem. Eng. J.*, 2010, **160**, 660–670.
- 73 F. Salak Asghari and H. Yoshida, *Ind. Eng. Chem. Res.*, 2006, **45**, 2163–2173.
- 74 P. Carniti, A. Gervasini, S. Biella and A. Auroux, *Catal. Today*, 2006, **118**, 373–378.
- 75 I. Jiménez-Morales, J. Santamaría-González, A. Jiménez-López and P. Maireles-Torres, *Fuel*, 2014, **118**, 265–271.
- 76 W. H. Hsu, Y. Y. Lee, W. H. Peng and K. C. W. Wu, *Catal. Today*, 2011, **174**, 65–69.
- 77 R. Van Putten, J. C. Van Der Waal, E. De Jong, C. B. Rasrendra, H. J. Heeres and J. G. De Vries, *Chem. Rev.*, 2013, **113**, 1499–1597.
- 78 R. Weingarten, G. A. Tompsett, W. C. Conner and G. W. Huber, *J. Catal.*, 2011, **279**, 174–182.
- 79 E. Nikolla, Y. Roman-Leshkov, M. Moliner and M. E. Davis, *ACS Catal.*, 2011, **1**, 408–410.
- 80 Q. Hou, X. Qi, M. Zhen, H. Qian, Y. Nie, C. Bai, S. Zhang, X. Bai and M. Ju, *Green Chem.*, 2021, **23**, 119–231.